Effects of Particle Shape and Size Distributions on the Electrical and Magnetic Properties of Nickel/Polyethylene Composites*

HALIT S. GÖKTÜRK, THOMAS J. FISKE, and DILHAN M. KALYON†

Highly Filled Materials Institute at Stevens, Castle Point on the Hudson, Hoboken, New Jersey 07030

SYNOPSIS

Electrical and magnetic properties of composite materials prepared by incorporating various nickel-based fillers of different shapes into polyethylene were investigated. The fillers used were nickel powders, nickel filamentary powders, nickel flakes, and nickel-coated graphite fibers. The particle-size distributions of the fillers were determined both before and after the processing of the composite samples. A wide range of filler volume fractions were used. In some cases, the volume fraction approached the maximum packing fraction of the solid phase to significantly exceed the percolation threshold. The composite samples were characterized in terms of their volume resistivity, dielectric constant, and magnetic permeability values. Filler particles of asymmetric shapes were very effective in terms of altering the electrical properties of the composite samples. At the highest loading levels of the nickel fillers, the volume resistivity values of the composites decreased by more than 17 orders of magnitude. At such high filler concentrations, the dielectric constant values of the composite samples increased considerably, to values that were greater than 1000. The permeability values of the samples increased linearly with the volume fraction of the nickel filler and were insensitive to the shape of the fillers. The highest relative permeability value measured was 5.8 for composites with 67% by volume of nickel powder. © 1993 John Wiley & Sons, Inc.

INTRODUCTION

Polymers are generally electrically insulating and nonmagnetic in nature. Both of these properties can be modified by the introduction of conducting and/or magnetic fillers into the polymer.[1,2] The main application for conductive composites is enclosures that can attenuate electromagnetic and radio-frequency interference (EMI/RFI). Conductive composites are also used in applications that require electrostatic dissipating parts, low power resistance heaters, and artificial dielectrics. Magnetic composites with a polymeric matrix offer ease of processing and shaping into three-dimensional shapes. Such composites can be processed and shaped using conventional methods of polymer processing including injection-molding. There are examples in the literature to permanent magnets prepared by mixing magnetic powders with polymeric matrices.[3]

THEORY

Filler Particles of Different Shapes

The filler material of a composite material can consist of spherical particles as in the case of powders or of particles of asymmetric shapes, like fibers or flakes. What kind of a filler geometry would be more advantageous in terms of altering the electrical and magnetic properties of the composite? Before proceeding to discuss the characteristics of a filled polymer, it is instructive to analyze the behavior of one isolated filler particle placed in an external electrical field. For generality, the shape of the filler particle can be chosen as an arbitrary ellipsoid. Let a conductive ellipsoid be placed in an initially uni-

* This paper is based on a presentation at the Annual Technical Conference of the Society of Plastics Engineers, Detroit, MI, May 1992.

† To whom correspondence should be addressed.

Journal of Applied Polymer Science, Vol. 50, 1891–1901 (1993)
 CCC 0021-8995/93/111891-11

form external electric field directed along the Cartesian axis, i. The conductive particle distorts the uniform field in its vicinity such that the electric field lines are normal to the surface of the ellipsoid and the electric field inside the conductor is zero. Figure 1 shows the field lines for the special case of a conductive sphere. The distortion of the uniform field decreases with increasing radial distance from the center of the ellipsoid. The solution of the electric potential, ψ, at points away from the ellipsoid is given as[4]

$$\Psi = -E_0 i + S_i(i/r^3), \quad i = x, y, \text{ or } z \qquad (1)$$

$$S_i = E_0 V/(4\pi n_i) \qquad (2)$$

where E_0 is the magnitude of the external electric field; S_i, the strength of the electric potential of the ellipsoid along the i-axis; and V, the volume of the ellipsoid. The parameter n_i is called the depolarizing factor and depends only on the shape of the object. As the ellipsoid is oriented at different directions with the respect to the external electric field, n_i assumes different values, changing the strength of the field induced due to the presence of the ellipsoid. To describe the influence of the shape factor further, three special classes of ellipsoids will be considered: a sphere, a prolate spheroid, and an oblate spheroid.

Sphere

Different orientations of a sphere with respect to an external field yield the same result, since the geometry of the sphere is uniform in all directions. It follows from this spherical symmetry that the depolarizing factors along different axes are equal. The sum of the depolarizing factors, n_x, n_y, and n_z is known to be unity for all ellipsoids.[4] Hence;

$$n_x = n_y = n_z = \tfrac{1}{3} \qquad (3)$$

The powder particles used in this study are generally in the form of small aspect ratios, and thus should approach the behavior of spherical filler particles.

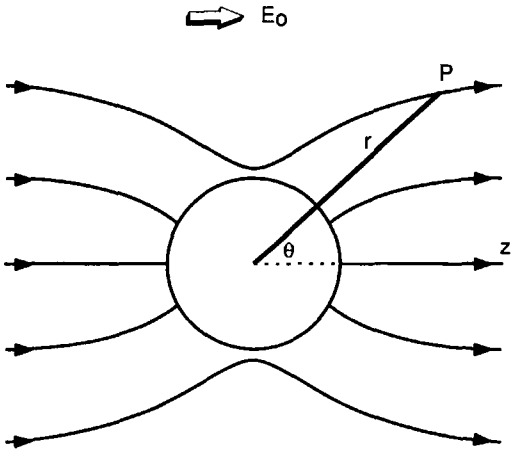

Figure 1 A conductive spherical particle placed in a uniform electric field, E_0.

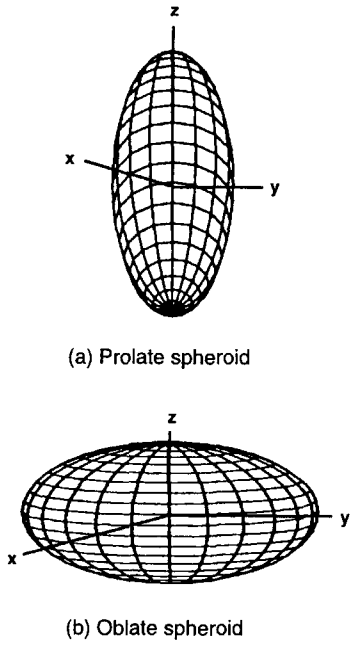

Figure 2 Two different spheroids that can be used to model assymetric filler particles.

Prolate Spheroid

A prolate spheroid is obtained by rotating an ellipse about its major axis [Fig. 2(a)]. A good example of this geometry is a football. The particles of a fibrous filler can also be represented as high aspect ratio prolate spheroids. Choosing the axis of symmetry, i.e., the major axis of the ellipse, along the z-direction, the depolarizing factors can be written as follows[4]:

$$n_z = \frac{1 - e^2}{2e^3}\left(\ln\frac{1+e}{1-e} - 2e\right) \qquad (4)$$

$$n_x = n_y = (1 - n_z)/2 \qquad (5)$$

$$e = [1 - (b^2/a^2)]^{1/2} \qquad (6)$$

b/a is the ratio of the minor axis to the major axis, which is the reciprocal of the aspect ratio. The strength, S_i, of the electric potential of the con-

ducting prolate spheroid can now be compared for two different orientations of the electric field. One orientation is chosen as parallel to the major axis, the z-axis, and the second one, as parallel to one of the minor axes, e.g., the x-axis.

$$S_z/S_x = n_x/n_z \tag{7}$$

For an aspect ratio of a/b equal to 10, S_z/S_x is 24. S_z/S_x increases rapidly with an increasing aspect ratio as shown in Figure 3. The strength of the potential of the prolate spheroid is enhanced considerably when the field is parallel to the long axis.

Oblate Spheroid

An oblate spheroid is obtained by rotating an ellipse about its minor axis [Fig. (2b)]. A good example to an oblate spheroid is a disk. The particles of a flake-type filler can be modeled as oblate spheroids. Choosing the axis of symmetry, i.e., the minor axis, along the z-direction, the depolarizing factors can be written as follows[4]:

$$n_z = \frac{1 + e^2}{e^3}\,[e - \arctan(e)] \tag{8}$$

$$n_x = n_y = (1 - n_z)/2 \tag{9}$$

$$e = [(a^2/b^2) - 1]^{1/2} \tag{10}$$

For an aspect ratio of a/b equal to 10, the ratio of the strength factor of one of the major axes to that of the minor axis, S_x/S_z, is 12.3. S_x/S_z is plotted in Figure 3 as a function of increasing aspect ratio from 2 to 1000. The ratio of strength factors for the oblate spheroid is smaller than that of the prolate spheroid at a given aspect ratio. However, the strength factors of the major axes of the oblate spheroid are significantly greater than that of a sphere of equal volume, even at modest aspect ratios. For example, at an aspect ratio of 10, the strength factor of the oblate spheroid can be calculated from eq. (3), (8), (9), and (10) to be 4.5 times that of the sphere. The oblate spheroid example also indicates that asymmetric shapes with large aspect ratios are the most desirable geometries for achieving high strength-factors.

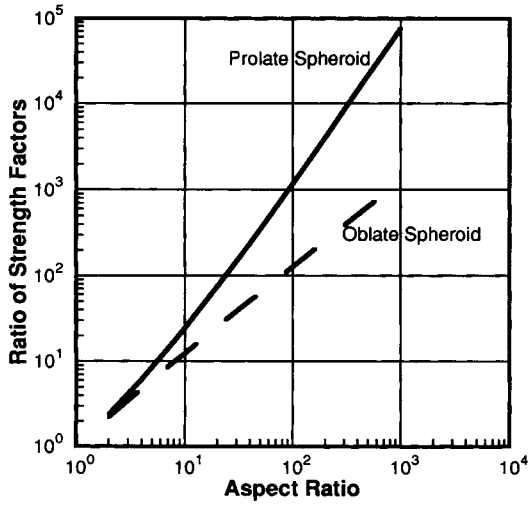

Figure 3 Ratio of the strength factor of the major axis to that of the minor axis for two different spheroids.

A similar problem can be formulated for the case of a single magnetic particle in a uniform magnetic field. If the relative permeability of the particle is very large, the governing equations and the corresponding boundary conditions become similar to that of the conducting particle in an electric field.[4] Therefore, the conclusions derived for the asymmetric conducting particles should also apply to asymmetric magnetic particles.

Interparticle Interaction

Let us now consider a filled polymer consisting of a collection of filler particles dispersed inside a polymeric matrix. The response of the filler particles of the composite to an applied external field depends on the average distance of separation between the nearest neighbors at a given volume fraction.[5] As can be noted from eq. (1), each particle placed in an external field generates a field of its own, given by the second term in eq. (1). This field decreases with increasing radial distance from the particle. At low volume fractions of the filler, the average separation between the nearest neighbors is such that the field of each filler particle at the position of the nearest neighbor is small in comparison to the external field. The filler particles act like isolated particles. In this regime, the properties of the composite change as a linear function of the filler volume fraction.[6] As the volume fraction increases, the filler particles approach each other and the interaction between the neighboring particles start to become significant. The interparticle interaction results in the enhancement of the electrical properties of the composite.[5-7] The properties start to vary at a higher rate than as a linear function of the volume fraction. Therefore, conductive filler particles are more effective in contributing to the development of the electrical properties of the composite when they are used at high loading levels.

Asymmetric filler particles provide an additional advantage in terms of the distance of separation. Results of percolation studies carried out with conductive particles in polymeric matrices indicate that asymmetric fillers establish conducting networks within the polymer at lower volume fractions than do powders.[8,9] Furthermore, the volume fraction at which the onset of conducting networks is attained decreases with an increasing aspect ratio.[9] These results suggest that the interparticle interaction between high aspect ratio asymmetric fillers would take place at lower concentrations than those of conductive filler particles with lower aspect ratio values.

OBJECTIVE

This study aimed to characterize the electrical and magnetic properties of composite materials consisting of nickel and nickel-coated particles of different shapes incorporated into polyethylene. Nickel was selected as the filler component because it was both electrically conductive and ferromagnetic. This selection allowed both electrical and magnetic properties to be simultaneously investigated. Three different shapes of the filler were used. Nickel fillers in the form of powders, filamentary powders, and flakes were utilized to compare the percolation properties of different shapes. A fourth filler investigated in this study was the nickel-coated graphite fiber. This filler served to provide information about whether the surface layer or the bulk of the filler is involved in contributing to the electrical and magnetic properties of the composite. The suspensions were prepared at various concentrations. High-volume loading levels including those that were close to the theoretical maximum packing fraction were emphasized to investigate the behavior of the filler particles at very small distances of interparticle separation. Furthermore, for comparison purposes, the properties of the composites containing different filler shapes were investigated at the constant volume fraction of 0.2. The particle-size distributions of the filler particles were characterized both before and after they were incorporated into the composite. The electrical and magnetic properties, which were measured, included volume resistivity, dielectric constant, and magnetic permeability.

EXPERIMENTAL

Material Preparation

The low-density polyethylene used in this study was Petrothene PEV 007 obtained from USI Chemicals, Cincinnati, OH. The nickel filamentary powder (type 287) and flakes (HCA-1) were procured from Novamet, Wyckoff, NJ, and the nickel-coated graphite fibers (DB-910–3) were obtained from American Cyanamid Co., Wallingford, CT. The nickel powder was supplied by Johnson Matthey of Ward Hill, MA.

The polyethylene/nickel composites were prepared in a Haake Rheocord Torque Rheometer System 40 with a Rheomix 600 mixing head attachment at 150°C and 60 rpm. The composite samples were molded using a Carver compression molder at 150°C and 2 MPa. Three samples were prepared for each concentration of the filler. The specimens prepared for electrical measurements were disks of 20 mm in diameter with thicknesses ranging from 1 to 3 mm. The surfaces of the samples were polished to remove the resin-rich layer and to eliminate surface irregularities. Contact electrodes were painted onto the measuring surfaces by means of a silver-filled polymer alloy, DY350, procured from Zymet, East Hanover, NJ. The specimens prepared for magnetic measurements were toroidal in shape. The dimensions of the toroid were outer diameter of 7.6 cm, inner diameter of 6.35 cm, and thickness of 0.635 cm. Two sets of windings were uniformly wrapped around the toroids: the first one to serve as the excitation coil, and the second one, as the sense coil. The average number of turns of the windings was 100.

Characterization

The particle-size distributions of the fillers were thoroughly characterized both before and after they were incorporated into the matrix. Particle-size analysis was carried out using a Joel scanning electron microscope (SEM) and a computerized quantitative image analysis technique. Samples of the nickel fillers were mounted on sample holders with conductive silver paint and they were sputtered with a thin layer of gold. The samples were scanned with the SEM at various magnifications. The micrographs produced were digitized by a frame grabber via a CCD linkup. The particle-size distributions were obtained using Image Analyst software from Automatix, Billerica, MA. For the composites, the above procedure was applied to all the samples at different concentrations after burning out the polyethylene matrix.

The experimental setup used to measure the volume resistivity of the samples consisted of a power supply as a voltage source, a picoammeter, Keithley, Model 485, and a computer, Macintosh IIfx, for au-

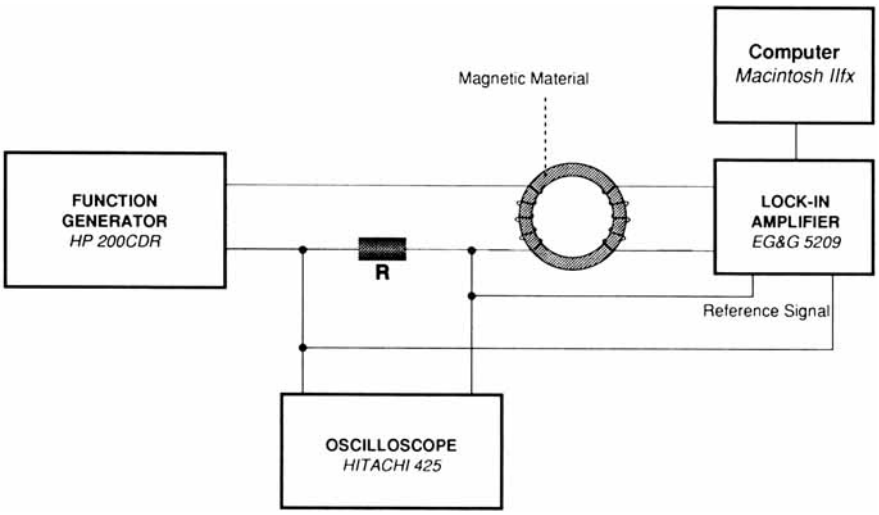

Figure 4 Magnetic permeability measurement setup.

tomated data collection and processing. The computer was equipped with data acquisition and IEEE 488 interface cards from National Instruments along with LabView software. The basic features of the setup conformed to ASTM standard designation D257–78, DC Resistance and Conductance of Insulating Materials .

The ac electrical property measured was the dielectric constant defined as the permittivity of a material medium divided by the permittivity of free space, ϵ_0. The key instrument in the measurement setup was a precision LCR meter, Hewlett-Packard Model 4284A, used in conjunction with a dielectric test fixture, Hewlett-Packard Model 16451B. The frequency range of the instrument was from 20 Hz to 1 MHz. The setup conformed to the ASTM standard designation D150–87, AC Loss Characteristics and Permittivity of Solid Insulating Materials . The LCR meter was connected to the data acquisition computer through an IEEE 488 interface.

The magnetic permeability measurement setup was designed in accordance with ASTM standard designation A772–80, AC Magnetic Permeability of Materials Using Sine Current (Fig. 4). The primary winding of the toroidal sample was excited with a sine wave from a function generator, Hewlett-Packard Model 200CDR. The voltage induced in the secondary winding was measured with a lock-in amplifier, EG&G Model 5209. The frequency range of the amplifier was from 0.5 Hz to 120 kHz. The lock-in amplifier was equipped with an IEEE 488 interface through which it was connected to the data ac-

Table I Particle-size Analysis of the Fillers (Powder, Flake, Filament, and Fibers)

Material	Filler Volume %	Length (μm)	Width (μm)	Diameter (μm)	Aspect Ratio	ϕ_m	V/n_i (μm)^3
Ni POWDER				110.0	1.0	0.682	
PE/Ni POWDER	20			74.5	1.0	0.680	636,590
PE/Ni POWDER	67			77.6	1.0	0.684	745,500
Flakes			1	13.7	13.7	—	
PE/Ni FLAKES	20		1	13.0	13.0	—	1,609
PE/Ni FLAKES	37		1	13.0	13.0	—	1,609
Filaments		15.0		1.0	15.0	0.300	
PE/Ni FILAMENTS	20	6.2		1.0	6.2	0.420	79
PE/Ni FILAMENTS	30	6.5		1.0	6.5	0.420	88
PE/Ni FILAMENTS	38	7.7		1.0	7.7	0.400	134
Fibers		5000.0		7.6	650.0	0.010	
PE/Ni FIBERS	5	122.0		7.6	16.0	0.290	761,360
PE/Ni FIBERS	20	85.5		7.6	11.2	0.340	303,630
PE/Ni FIBERS	26	80.4		7.6	10.6	0.340	262,200

quisition computer. A toroidal sample molded of neat polyethylene was used as a reference sample. The relative permeability values were obtained by comparing the voltage induced in the secondary winding of composite samples with that of the reference sample.

RESULTS AND DISCUSSION

Particle-size Distributions

The results of the particle-size analyses are summarized in Table I along with the aspect ratios, the estimated maximum packing fractions, ϕ_m, and volume/depolarizing factors (V/n_i) calculated from eq. (3–6) and (8–10). Where available, the results are shown with the 95% confidence intervals of the Student's-t-distribution. The Novamet filamentary powder has a bead-and-chain structure. The beads have a diameter of 1 micron and the chains have a length of 15 microns. The nickel flakes have an average thickness of 1 micron and a diameter of 13.7 microns. The nickel-coated graphite fibers have an average diameter of 7.6 microns and are approximately 5 mm in length. These fibers contain 60% nickel and 40% graphite by weight. The nickel powder has an average diameter of 110 microns with an aspect ratio that is close to 1. The scanning electron micrographs of the filler materials are shown in Figures 5 and 6.

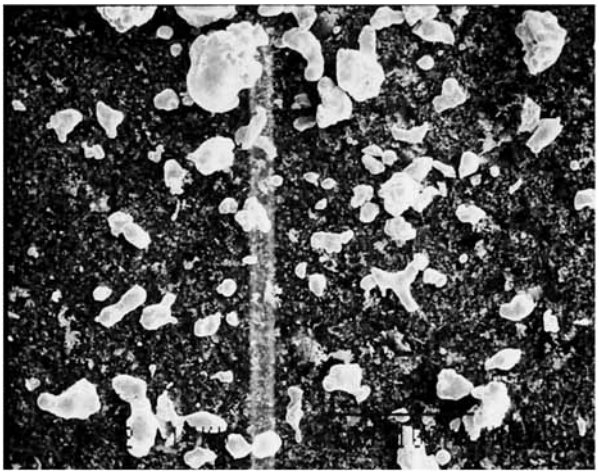

(a)

(b)

Figure 5 Scanning electron micrographs of (a) nickel powders and (b) nickel flakes.

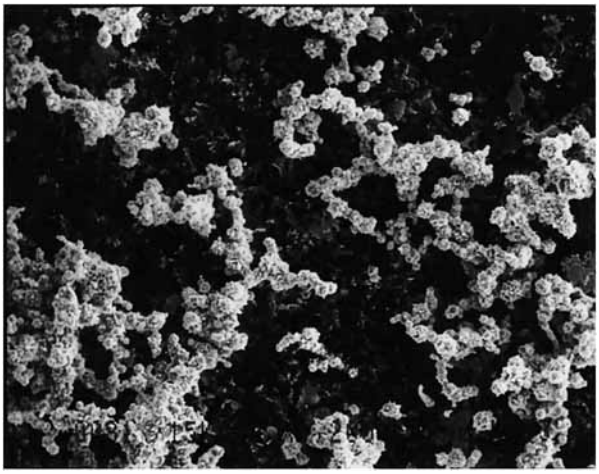

(a)

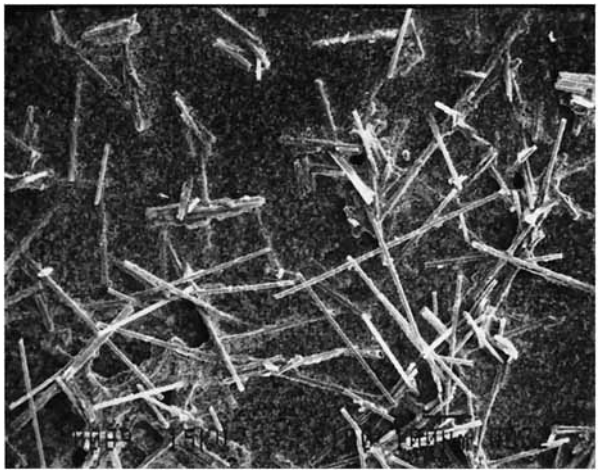

(b)

Figure 6 Scanning electron micrographs of (a) nickel filamentary powders, (b) nickel-coated graphite fibers.

The particle-size distributions of nickel powder samples are shown in Figure 7. The results of the measurements indicate that the processing caused larger particles to break up into smaller ones. The number-average diameter for nickel powder before mixing was 110 μm, while after processing, it decreased to approximately 75 μm. The aspect ratio for all the powder particles remained approximately 1. The number-average diameter values for the powder samples, corresponding to different concentrations used in the composite samples are listed in Table I. The estimated maximum packing fraction values given in Table I are calculated using the method of Poslinski et al.[10]

Figure 8 shows the particle-size distributions for nickel flake samples. The results reveal that the

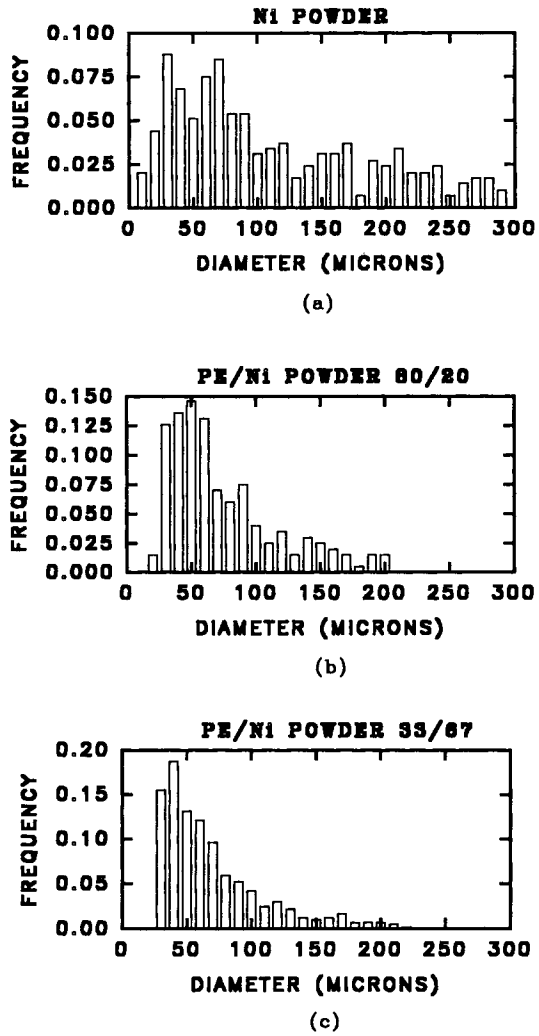

Figure 7 Particle-size distribution of nickel powder (a) before mixing, (b) from composites containing 20% filler by volume, and (c) from composites containing 67% filler by volume.

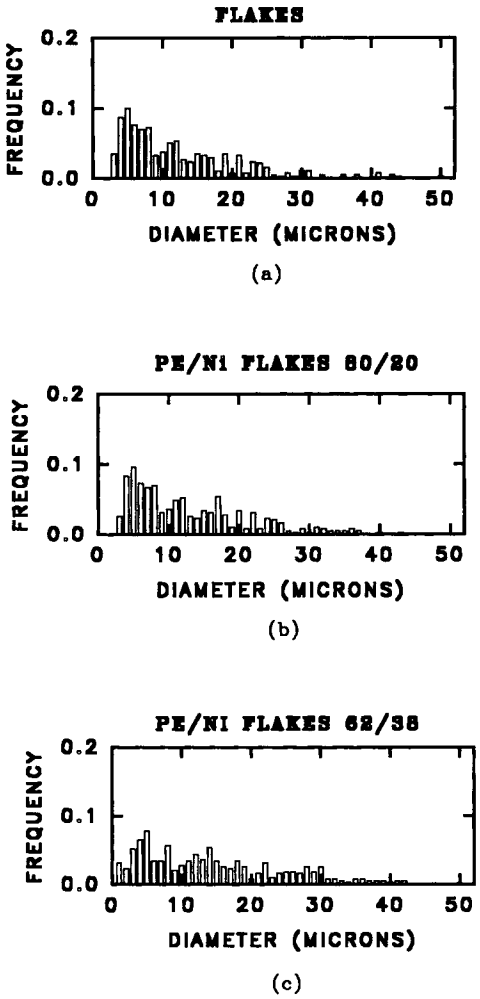

Figure 8 Particle-size distribution of nickel flakes (a) before mixing, (b) from composites containing 20% filler by volume, (c) from composites containing 38% filler by volume.

flakes did not degrade upon mixing but maintained their original shapes and sizes. The number-average diameter and the average thickness of the flake-shaped particles were about 13 and 1 μm, respectively. Thus, the average aspect ratio of the flake-shaped nickel filler was 13.

Particle-size distributions for the filamentary powder samples are shown in Figure 9. The average values listed in Table I indicate that the filamentary powders broke up during processing. The average length deteriorated to about half its initial value, i.e., decreased from approximately 15 μm initially to values between 6.2 and 7.5 μm upon processing. The estimated maximum packing fraction values listed in Table I for the filamentary powders are based on the work of Milewski for high aspect ratio fibers.[11]

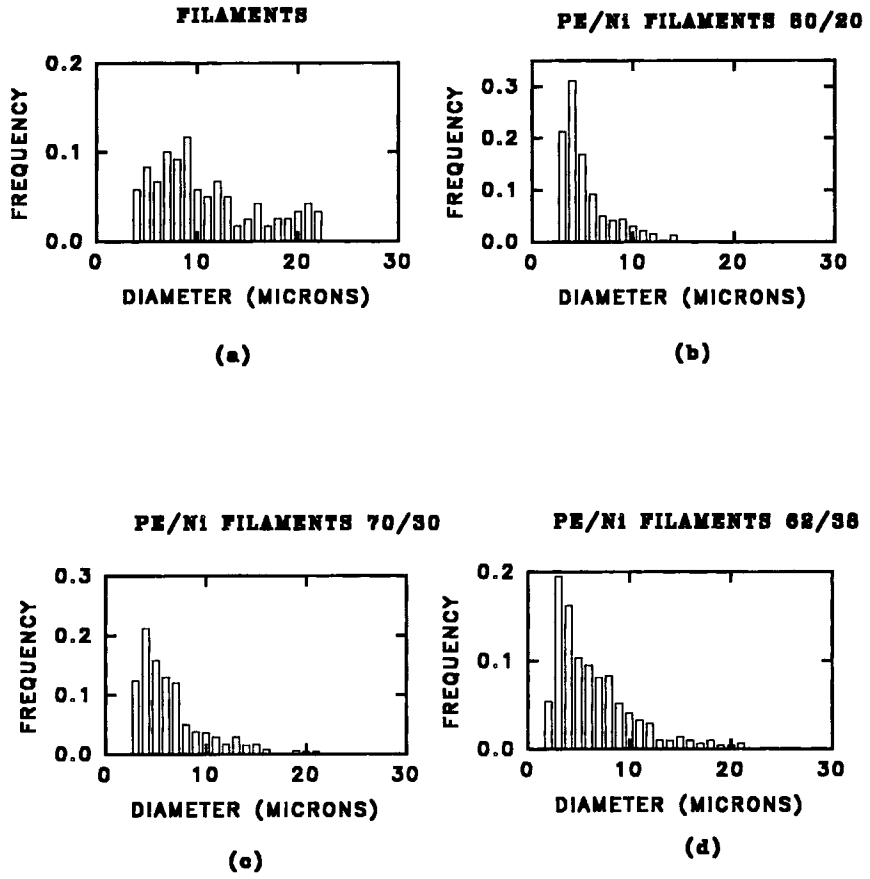

Figure 9 Particle-size distribution of nickel filamentary powder (a) before mixing, (b) from composites containing 20% filler by volume, (c) from composites containing 30% filler by volume, and (d) from composites containing 38% filler by volume.

The particle-size distributions of the nickel-coated graphite fiber samples are shown in Figure 10 and the number-average lengths are listed in Table I. Upon processing, the average length of the nickel-coated graphite fibers degraded by more than one order of magnitude. At the volume fraction of 0.2, the average length of the nickel-coated graphite fibers was measured as 85.5 μm. This value is greater than the characteristic dimension of the flakes at the same volume fraction, 13 μm. However, the initial high aspect ratio of the nickel-coated graphite fibers reduced to values comparable to those of the flakes (11.2 for nickel-coated graphite fibers vs. 13 for the flakes) upon processing.

Volume Resistivity

The volume resistivity of neat polyethylene was measured to be outside the range of the experimental setup. This result was expected from the typical values of the volume resistivity of polyethylene reported in the literature, i.e., around 10^{20} ohm-m.[12] The results listed in Table II indicate that the volume resistivity values decreased very sharply with the addition of conductive fillers at loading levels that approached the maximum packing concentrations. At the highest levels of loading employed, the volume resistivity values became too small to be accurately measured with our experimental setup. At the volume fraction of 0.2, there was a four orders of magnitude difference between the volume resistivity values of composite samples incorporated with the nickel powder and the nickel filamentary powder. Nickel-coated graphite fibers, which had the highest initial aspect ratios of all the fillers, altered the electrical conductivity of the composite substantially even at volume fractions of 0.05. The conductive surface layer of the nickel-coated graphite fiber was sufficient to achieve electrical percolation. Similar trends were observed with nickel-coated graphite fibers incorporated into other polymers.[13]

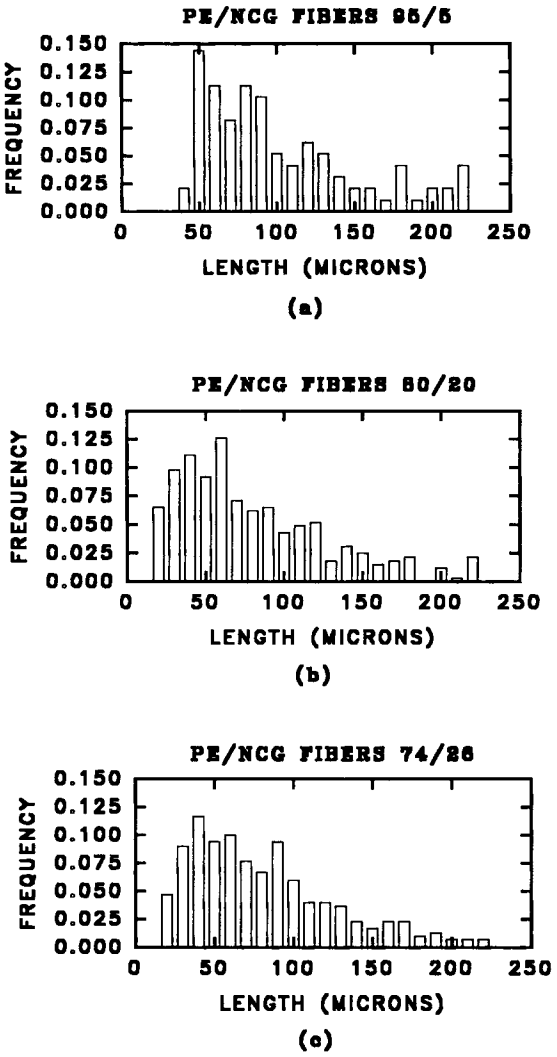

Figure 10 Particle-size distribution of nickel-coated graphite fibers from composites containing (a) 5% filler by volume, (b) 20% filler by volume, and (c) 26% filler by volume.

Dielectric Constant

The dielectric constant of polyethylene was measured to be 2.4 ± 0.1. This value agrees with the typical values reported in the literature.[12] The dielectric constant values increased with increasing conductive filler content of the composite as shown in Table II. This increase is primarily due to the electrical polarization associated with the charges induced on the surfaces of the metallic filler particles. At the volume fraction of 0.2, composite samples containing powder fillers exhibited the lowest dielectric constant values. At the same loading level, the dielectric constant of composites with filamentary powder and flake-type fillers increased with increasing aspect ratio.

The enhancement of the dielectric constant at higher aspect ratios is believed to be due to the formation of clusters of the filler particles. In accordance with the teachings of the percolation theory, as the concentration of the filler particles is increased from very low values to the percolation threshold, first adjacent filler particles form small connected lattice locations, i.e., clusters; next, these isolated clusters start to increase in size; and, finally, the neigboring clusters make contact, establishing a conductive network.[14] Higher aspect ratios facilitate the formation of clusters and, thereby, lower the threshold concentration.[9] The average electrical polarization associated with a cluster is larger than that of an individual particle because of the increase in the dimensions of the conductive inclusion. A comparison of the dielectric constant values of these composites with the volume/depolarizing factors (V/n_i) given in Table I indicate that there is not a good correlation. This result suggests that the dielectric properties of the composite were significantly influenced by the collective behavior of the filler particles at the concentrations used in the experiments.

The frequency dependence of the dielectric constant was also measured in the range 100 Hz to 1 MHz and the results of the measurements are shown in Figure 11. The dielectric constant values of the composite samples incorporated with asymmetric fillers exhibited a strong dependence on frequency, increasing substantially at low frequencies. The significant enhancement of the dielectric constant values at low frequencies is again believed to be due to the clusters of the filler particles in the composite. At low frequencies, the surface charges that contribute to the electrical polarization have more time to rearrange themselves on the clusters that have relatively larger dimensions, generating greater polarizations.

Magnetic Permeability

Results of relative permeability measurements, listed in Table II, indicate very different trends than what was observed with electrical properties. The changes observed in the relative permeability values by the addition of the ferromagnetic fillers were incremental. The highest relative permeability value obtained was 5.8 for the composite samples containing 67% by volume of nickel powder. At the volume fraction of 0.2, the relative permeability values

Table II Electrical and Magnetic Properties of Nickel-filled Polyethylene

Filler Material[a]	Filler Volume Fraction	Volume Resistivity (Ω-m)	Dielectric Constant[b]	Relative Permeability[c] (±0.05)
Ni powder	0.20	$(6 \pm 0.4) \times 10^9$	7.9 ± 0.2	2.17
	0.67	< 0.05	> 1000	5.80
Ni filaments	0.20	$(1.7 \pm 0.7) \times 10^5$	25.6 ± 6	2.10
	0.30	$(3.4 \pm 0.8) \times 10^3$	190 ± 6	2.57
	0.38	< 0.05	> 1000	3.45
Ni flakes	0.20	$(1.3 \pm 1) \times 10^5$	144 ± 4	2.04
	0.37	< 0.05	> 1000	3.26
NCG fibers	0.05	< 0.05	> 1000	1.24
	0.20	< 0.05	> 1000	1.38
	0.26	< 0.05	> 1000	1.44
Polyethylene	—	$> 10^{15}$	2.4 ± 0.1	1.00

[a] Ni: nickel; NCG: nickel-coated graphite.
[b] Measured at 100 kHz, 300 V/m.
[c] Measured at 1 kHz, 360 A/m.

exhibited by samples incorporated with different types of fillers were comparable. This result suggests that the shape of the filler particles did not play a role in terms of influencing magnetic permeability. The highest relative permeability value was obtained for composite samples containing the largest volume fraction of nickel and the lowest values were associated with nickel-coated graphite fibers containing the smallest concentration of nickel. The permeability values are plotted in Figure 12 as a function of the volume fraction of the nickel in the composite. The permeability values increase linearly with increasing nickel concentration. Frequency variation of the relative permeability values of the composite samples was also investigated. Results plotted in Figure 13 indicate that, unlike the dielectric constant values of these composites, the magnetic permeability values are insensitive to frequency in the measurement range from 10 Hz to 100 kHz.

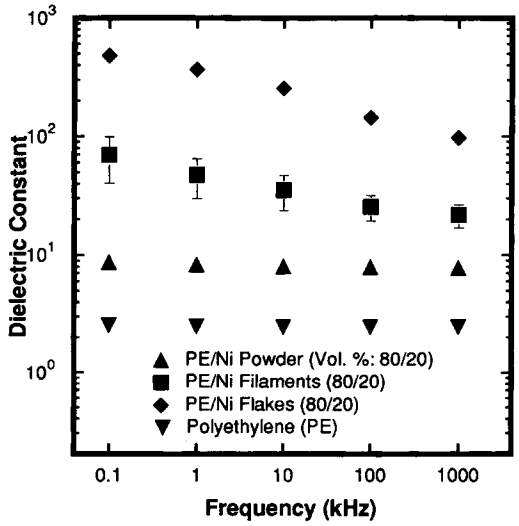

Figure 11 Frequency variation of the dielectric constant values of the composite samples; measured at 300 V/m.

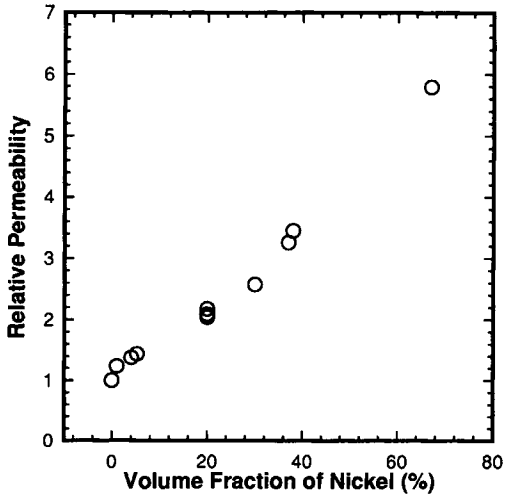

Figure 12 The variation of permeability values of the composite samples with the nickel concentration; measured at 1 kHz and 360 A/m.

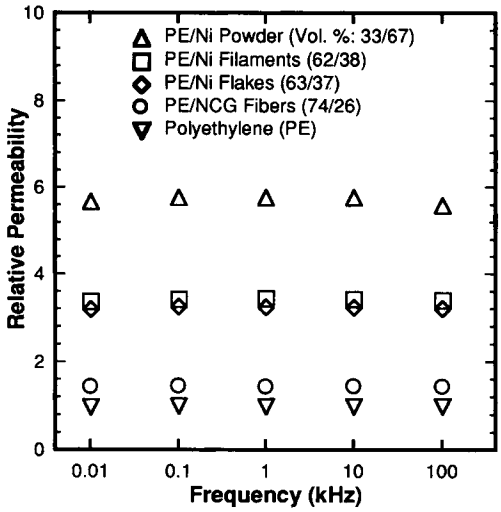

Figure 13 Frequency variation of the relative permeability values of the composite samples; measured at 360 A/m.

CONCLUSIONS

The properties of nickel and nickel-coated fillers incorporated into polyethylene composites were studied. Four types of fillers with different shapes, i.e., low aspect ratio powders, filaments, flakes, and graphite fibers coated with nickel were used. The size distributions of the fillers were characterized. Upon processing, a reduction was observed in both the size and aspect ratio of the filler particles. At loading levels that were close to the maximum packing fraction, the volume resistivity values of the composite materials decreased more than 17 orders of magnitude with respect to neat polyethylene. The fiber and flake-shaped fillers were more effective in decreasing the electrical resistivity in comparison to spherical powders, inducing greater changes in the electrical properties at comparable volume concentrations. Among the asymmetric fillers, the highest aspect ratio nickel-coated graphite fibers required the smallest loading levels to generate electrical percolation. The dielectric constant values of the composite materials were significantly enhanced upon the addition of the conductive fillers. The composite samples with higher aspect ratio fillers gave rise to greater dielectric constant values. The magnetic permeability values of the composite samples increased linearly with increasing nickel concentration. The highest relative permeability value measured was 5.8 for samples that contained 67% by volume of nickel powder. The permeability values were not affected by the shape of the filler particles. The frequency variation of the properties were also investigated in the range of 10 Hz to 1 MHz. The magnetic permeability values of the composites remained insensitive to frequency, whereas the dielectric permittivity values increased significantly at low frequencies.

We gratefully acknowledge the contributions of Novamet for supplying the nickel filaments and flakes for this study. We thank the American Cyanamid Co. for providing the nickel-coated graphite fibers.

REFERENCES

1. A. T. Ponomarenko, V. G. Shevchenko, and N. S. Enikolopyan, in *Advances in Polymer Science*, N. S. Enikolopyan, Ed., Springer-Verlag, Berlin, 1990, Vol. 96.
2. H. Stäblein, in *Ferromagnetic Materials*, E. P. Wohlfart, Ed., North-Holland, New York, 1986, Vol. 3.
3. T. Sakai, K. Nakamura, and A. Morii, *Int. Polym. Proc.*, **6**, 26 (1991).
4. L. D. Landau, E. M. Lifshitz, and L. P. Pitaevskii, *Electrodynamics of Continuous Media*, 2nd ed., Pergamon Press, New York, 1984.
5. H. S. Göktürk, T. J. Fiske, and D. M. Kalyon, *IEEE Trans. Mag.*, to appear
6. W. T. Doyle, *J. Appl. Phys.*, **49**, 795 (1978).
7. W. T. Doyle and I. S. Jacobs, *Phys. Rev. B*, **42**, 9319 (1990).
8. J. S. Sun, H. S. Göktürk, and D. M. Kalyon, *J. Mater. Sci.*, **28**, 364 (1993).
9. D. M. Bigg, *Adv. Polym. Tech.*, **4**, 255 (1984).
10. A. J. Poslinski, M. E. Ryan, R. K. Gupta, S. G. Seshadri, and F. J. Frechette, *J. Rheol.*, **32**, 751 (1988).
11. J. V. Milewski, *Ind. Eng. Chem. Prod. Res. Dev.*, **17**, 363 (1978).
12. J. A. Brydson, *Plastic Materials*, 5th ed., Butterworth, Boston, 1989.
13. M. E. Weber and M. R. Kamal, *Soc. of Plast. Eng. ANTEC Tech. Pap.*, **38**, 484 (1992).
14. S. Kirkpatrick, *Rev. Mod. Phys.*, **45**, 574 (1973).

Received December 31, 1992
Accepted April 13, 1993